Self-Renewal, Multipotency, and the Existence of Two Cell Populations within an Epithelial Stem Cell Niche

Cedric Blanpain,[1] William E. Lowry,[1]
Andrea Geoghegan, Lisa Polak, and Elaine Fuchs*
Howard Hughes Medical Institute
The Rockefeller University
New York, New York 10021

Summary

In adult skin, each hair follicle contains a reservoir of stem cells (the bulge), which can be mobilized to regenerate the new follicle with each hair cycle and to reepithelialize epidermis during wound repair. Here we report new methods that permit their clonal analyses and engraftment and demonstrate the two defining features of stem cells, namely self-renewal and multipotency. We also show that, within the bulge, there are two distinct populations, one of which maintains basal lamina contact and temporally precedes the other, which is suprabasal and arises only after the start of the first postnatal hair cycle. This spatial distinction endows them with discrete transcriptional programs, but surprisingly, both populations are growth inhibited in the niche but can self-renew in vitro and make epidermis and hair when grafted. These findings suggest that the niche microenvironment imposes intrinsic "stemness" features without restricting the establishment of epithelial polarity and changes in gene expression.

Introduction

Stem cells (SCs) have the unique capacity to self-renew and to differentiate into the cell lineages that constitute their tissue of origin. SCs are found in many adult tissues, including epidermis, intestine, muscle, the hematopoetic system, and even brain (Weissman et al., 2001; Wagers and Weissman, 2004). Within the tissue, they often reside in niches that provide a specialized environment thought to regulate their proliferation and differentiation (Spradling et al., 2001; Lin, 2002; Fuchs et al., 2004). SCs are critical for replenishing and maintaining the balance of cells (homeostasis) within the tissue and for regenerating tissue damaged during injury.

In skin, each unit of epithelium contains a hair follicle and its surrounding epidermis. The epidermis maintains homeostasis by proliferation of a single inner (basal) layer of mitotically active cells. As basal cells detach from their underlying basal lamina, they stop dividing, commit to terminally differentiate, and eventually are sloughed from the skin surface (Watt, 2002; Fuchs and Raghavan, 2002). Interfollicular epidermis maintains this balance for extended periods in the absence of injury. Like most stratified epithelia, it is thought to contain resident SCs attached to an underlying basal lamina and

embedded in a cluster of basal epidermal cells (Potten, 1974; Potten and Morris, 1988).

An appendage of mammalian epidermis, the hair follicle is composed of concentric rings of an external outer root sheath (ORS) attached to the basal lamina and contiguous with epidermis, a channel (inner root sheath, IRS), and finally the hair shaft (reviewed by Panteleyev et al. [2001]). The hair and its channel grow from the base (bulb) of the follicle, which contains committed but proliferating progenitor cells (matrix) encasing a cluster of specialized mesenchymal cells (dermal papilla, DP). When matrix cells undergo apoptosis, hair growth (anagen) ceases, and the lower half of each follicle degenerates (catagen). After a rest period (telogen), a stimulus involving the DP signals follicle epithelial cells at the base to initiate the regeneration of the lower follicle and produce a new hair (Jahoda et al., 1984). The new follicle develops adjacent to the old one, necessitating a reorganization of the regenerating cell progenitors at the follicle base, creating a bulge in the ORS. In mice, the bulge forms concomitantly with the initiation of this first postnatal hair cycle at approximately 3 weeks of age.

Several lines of evidence suggest that epithelial SCs reside in the bulge. Pulse-chase experiments with labeled nucleotides (Cotsarelis et al., 1990; Morris and Potten, 1999; Taylor et al., 2000) or transgenic expression of a fluorescent histone protein (Tumbar et al., 2004) marks the bulge as the residence of >95% of skin's infrequently cycling, label-retaining cells (LRCs) (Panteleyev et al., 2001). A wound stimulus prompts upward migration of marked bulge cells, whereas mesenchymal-epithelial interactions at the start of the hair cycle stimulate downward movement (Taylor et al., 2000; Tumbar et al., 2004; Morris et al., 2004). When cultured in vitro, bulge keratinocytes yield larger colonies than those from other skin sites (Rochat et al., 1994; Oshima et al., 2001; Tumbar et al., 2004; Morris et al., 2004). Finally, when marked rodent bulge cells are transplanted onto athymic mice, their progeny can be detected in the resulting epidermis, hair follicles, and sebaceous glands (Oshima et al., 2001; Morris et al., 2004). Whether the bulge contains multiple types of unipotent SCs or whether SCs within the bulge are multipotent and contribute to all of these keratinocyte lineages is still unclear and awaits clonal analyses of individual bulge cells.

Recently, enriched bulge populations were isolated from skin (Tumbar et al., 2004; Morris et al., 2004). These methods relied on the generation of transgenic mice that fluorescently marked bulge cells on the basis either of their infrequently cycling, label-retaining properties (Tumbar et al., 2004) or bulge-preferred promoter activity of the keratin 15 (K15) gene (Morris et al., 2004). Microarray analyses revealed ~150 mRNAs that were upregulated by greater than or equal to two times in bulge cells relative to a subset of integrin-positive progeny residing within the epidermal or contingent ORS basal layers.

By defining bulge cell characteristics, new avenues have been opened for probing more deeply into the cellular architecture and potential heterogeneity of skin

*Correspondence: fuchslb@rockefeller.edu
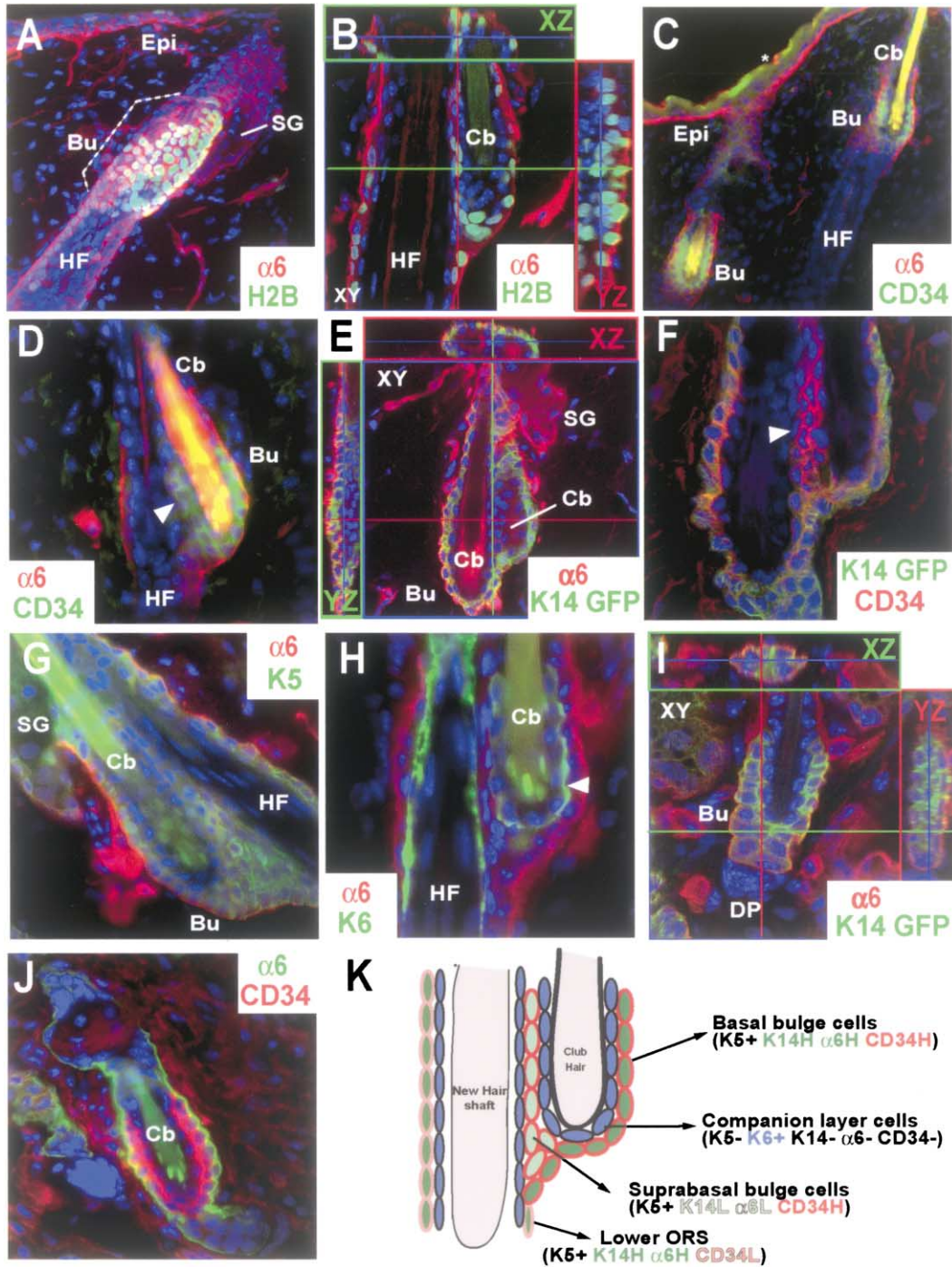[1]These authors contributed equally to this work.

Figure 1. The Formation of a Suprabasal Layer in the Skin Epithelial Stem Cell Niche

(A and B) Skin is from 9 week VP16Tet^off/TRE-H2B-GFP mice fed for the last 5 weeks on doxycycline (chase). Following immunofluorescence (antibodies or epifluorescence markers are color coded; counterstaining of nuclei is with either TOPRO3 or DAPI in blue), a three-dimensional reconstruction was assembled from 80 serial 0.5 μm confocal sections. Note LRCs (green) in anagen phase hair follicle (HF) bulge (Bu), located just below the sebaceous gland (SG). Section in (B) is through center of the bulge (X) with its Z (XZ, green box in upper panel) and Y projections (YZ, red box in right panel). Note existence of suprabasal LRCs in XZ and YZ projections. Epi, epidermis; Cb, club hair.

(C and D) Skin is from 28 day (d28) WT mouse, showing anti-CD34 staining in bulge of anagen phase follicle. Arrowhead points to CD34^+ suprabasal layer. Note: the epidermal granular layer often displayed artifactual fluorescence (asterisk), not dependent upon the primary antibodies used.

(E and F) Skin is from a 7 week K14-GFP-actin mouse, showing telogen phase bulge. Note: between old and new hairs are suprabasal bulge cells typified by low α6-integrin (red), K14 GFP-actin (green), and high CD34 (F) (arrowhead).

(G and H) Anagen phase bulge (28 day) showing K5 in basal and suprabasal compartments but not in the K6^+ companion layer of cells surrounding the old club hair shaft (arrowhead).

(I and J) Early anagen, day 20 follicles from K14-GFP-actin (I) or WT mice (J). At this stage, the bulge is still symmetrical, consisting of one α6^+CD34^+ layer that surrounds the CD34^-K6^+ companion layer of the old club hair.

(K) Schematic summarizing immunofluorescence patterns. L, low; H, high; +, present; −, absent.

SCs within their natural residence. To this end, we have now uncovered an asymmetry that first develops postnatally within the stem cell niche as it is mobilized to regenerate the hair follicle. At this time, the bulge becomes endowed with two distinct populations of resident cells, one attached and one detached from the basal lamina of extracellular matrix (ECM).

We devised a method to isolate the two bulge populations by fluorescence-activated cell sorting (FACS) and examine their behavior and molecular properties. We show that, within the niche, both populations remain quiescent, but in vitro, cells from each population can be induced to undergo SC self-renewal. Furthermore, by optimizing conditions that permit clonal analyses in vitro and engraftments in vivo, we show that both populations contain SCs, which are multipotent, able to differentiate into all lineages of epidermis and hair. Remarkably, this even includes formation of a structure within the follicle that shares some morphological and biochemical features of the follicle SC niche.

By analyzing the underlying biochemical differences of these bulge residents during both resting and growing phases of the hair cycle, we have been able to categorize features of bulge cells into those that are likely intrinsic to their stemness: those dependent upon attachment to basal lamina and those acquired upon detachment. These differences provide the first insights into how the microenvironment of the niche is able to impose SC behavior and restrict proliferation and irreversible commitment and yet remain permissive for changes in gene expression and cell polarity that are likely to be prerequisite to lineage differentiation.

Results

Asymmetry within the Follicle SC Niche

Mitotic activity, differentiation status, and morphogenesis in most epithelial cells are influenced heavily by associated basal lamina (Werb, 1997; Martin et al., 2002; Watt, 2002). To assess the relation between LRCs and their surrounding basal lamina, we conducted three-dimensional analyses of 40 μm thick frozen sections of skin from anagen phase, K5-VP16Tet^{off}/TRE-H2B-GFP transgenic mice (Tumbar et al., 2004) that were fed tetracycline for 5 weeks beginning at 1 month of age. At this time, only the nuclei of bulge cells retain high levels of H2B-GFP (Figure 1A). When sections were counterlabeled with antibodies against α6 integrin, a component of the hemidesmosomes that mediate attachment to the basal lamina (Martin et al., 2002; Watt, 2002), it was evident that, although many bulge LRCs contacted this substratum, others appeared to be suprabasal, irrespective of image plane (Figure 1B). This was most apparent on the side of the bulge where the new hair follicle (HF) emerged.

Antibodies against CD34, an established marker of both hematopoietic and skin epithelial SCs (Ramalho-Santos et al., 2002; Ivanova et al., 2002; Tumbar et al., 2004; Morris et al., 2004), stained both basal and suprabasal bulge cells (Figures 1C and 1D). Antibodies against the typically basal marker K14 (data not shown) as well as a K14 promoter-driven GFP-actin transgene (shown) also labeled both populations, although su-

prabasal cells were less bright (Figures 1E and 1F). Expression of another typically basal keratin, K5, was strong in both compartments (Figure 1G). By contrast, the companion layer surrounding the remnant hair shaft was negative for K14 and K5 but strongly positive for the typically suprabasal keratin K6 (Figure 1H).

At the end of the first telogen (d20), the follicle niche was symmetrical, consisting of a single layer of CD34$^+$ basal cells (Figures 1I and 1J). As anagen began (d22), the suprabasal compartment emerged concomitantly with the bulge. Once formed, both compartments were maintained throughout this and subsequent hair cycles. Figure 1K summarizes these results.

To further characterize CD34$^+$ bulge LRCs, we subjected single cell suspensions of skin to FACS on the bases of H2B-GFP retention and binding to α6 integrin and CD34 antibodies. Two populations of skin epithelial cells retained high H2B-GFP and displayed high surface CD34 but differed in surface α6 integrin (Figures 2A and 2B). Consistent with our immunofluorescence data, α6-low CD34-high (α6^{low}CD34^{high}) cells did not appear before the beginning of the first postnatal hair cycle but persisted thereafter (Figure 2D). α6^{low}CD34^{high} cells expressed ten times less GFP-actin and β1 integrin than α6^{high}CD34^{high} cells (Figures 2E and 2F). Both expressed ORS markers K5 and K15 but not appreciable differentiation markers for epidermis (K1), companion layer (K6), or IRS (AE15) (Figure 2F, cytospin).

Both Basal and Suprabasal Bulge Cells Can Be Stimulated to Self-Renew and Terminally Differentiate In Vitro

When epidermal keratinocytes detach from their underlying basal lamina, they terminally differentiate (Watt, 2002). To assess whether the suprabasal status might commit some bulge cells to irreversibly differentiate, we examined their potential to generate keratinocyte colonies in vitro. FACS was used to isolate pure populations of K14-GFP-actin expressing α6^{low}CD34^{high}, α6^{high}CD34^{high}, α6^{low}CD34$^-$, α6^{high}CD34$^-$, and GFP$^+$ keratinocytes from postnatal d28 mouse back skins (see Figure 2D).

In vitro, primary cultures of these FACS-isolated keratinocytes formed colonies with similar efficiencies (Figures 3A and 3B). However, only the α6^{low}CD34^{high} and α6^{high}CD34^{high} populations formed appreciable numbers of tightly packed, large colonies (>20 mm^2; >10^4 cells) containing cells of small size and relatively undifferentiated morphology (Figures 3A–3D). Referred to as holoclones, such colonies are clonally derived from single SCs (Barrandon and Green, 1987). Although the number of α6^{high}CD34^{high}-derived holoclones was higher, the ability of α6^{low}CD34^{high} cells to generate holoclones was unexpected, given their suprabasal location. By contrast, keratinocytes residing outside the bulge typically generated <5 mm^2 colonies, and even the larger colonies often displayed irregular borders and consisted of bigger, morphologically differentiated cells (Figures 3A and 3D). The holoclone-forming ability of our FACS-isolated, adult bulge keratinocytes was interesting in light of the fact that adult mouse keratinocytes have been difficult to culture long-term. In this regard, adult bulge cells resembled newborn and embryonic skin keratinocytes,
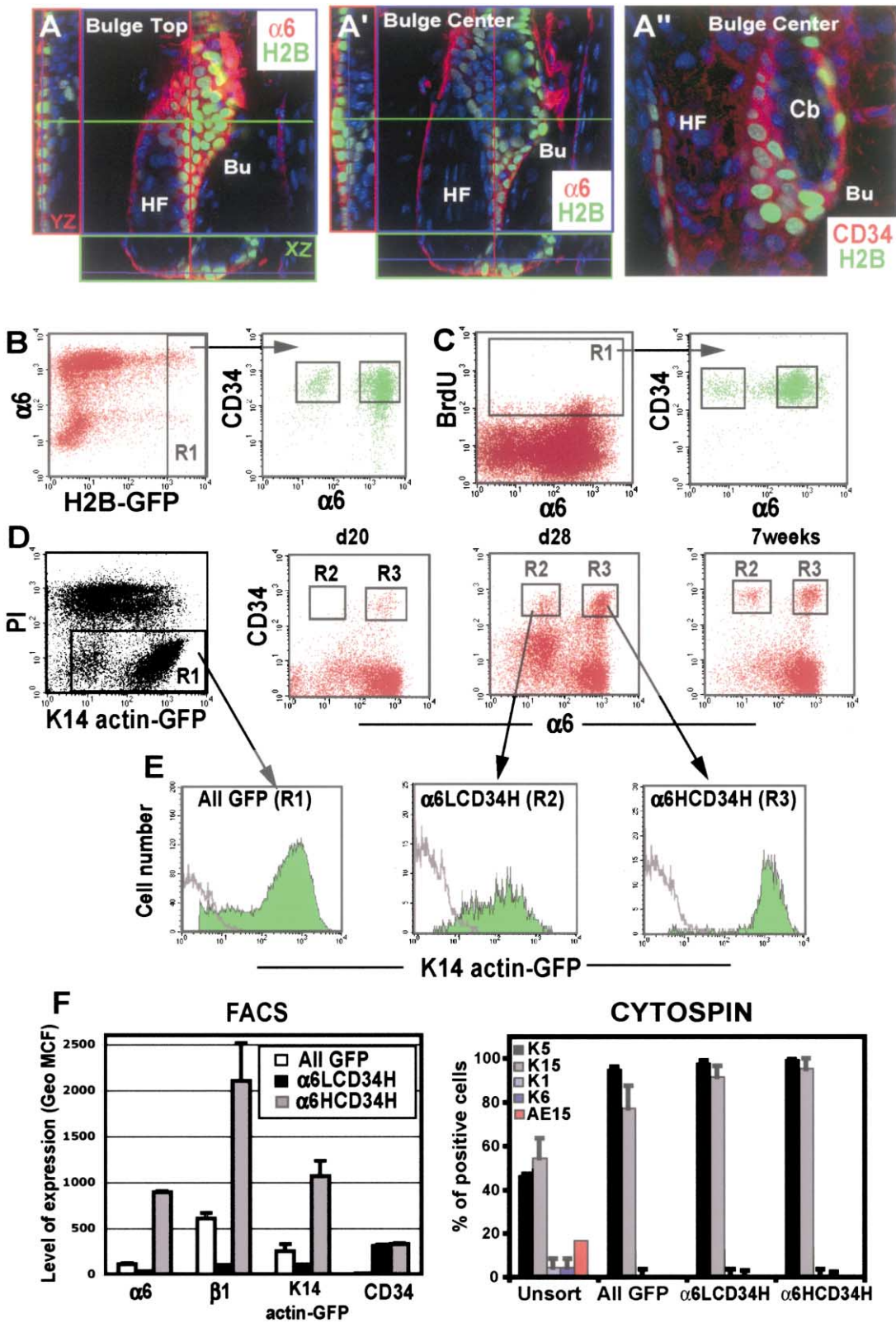
Figure 2. Isolation of Basal and Suprabasal Bulge Compartments on the Basis of CD34, α6 Integrin, and K5/K14 Promoter Activities

(A–A″) Confocal sections through top or center of bulge (XY) follicle from 28 day labeled, 28 day chased, K5VP16Tet^{off}, TRE-H2B-GFP mouse. Projections through Y (red box in left panel, YZ) and X axes (green box in lower panel XZ) are depicted at left and bottom of frames in (A)–(A′) to illustrate suprabasal LRCs (green).

(B) FACS analyses of cells from chased skin. FACS encompasses GFP epifluorescence and surface expression of α6 integrin and CD34, revealing two distinct LRC populations.

which form holoclones readily. In addition, the proliferation was greater for cells of the bulge than for their epidermal counterparts, both in short-term (Figure 3E) and in long-term (Figure 3G) culture.

To assess the ability of single bulge cells to undergo self-renewal, we conducted clonal analyses by trypsinizing and passaging cells derived from individual holoclones (Figure 3F). Colonies derived from representative $\alpha6^{low}CD34^{high}$ and $\alpha6^{high}CD34^{high}$ cells uniquely withstood multiple passages to yield new holoclones. This result indicates that both bulge populations contain cells that display the morphological and self-renewal features of SCs when taken outside of their native niche and exposed to proliferation-inducing conditions. The data also suggest that, if bulge cells enter early commitment upon detachment from basal lamina, this process is still reversible, at least in vitro.

Conversely, when keratinocytes derived from either of the two bulge compartments were induced to terminally differentiate in vitro, both populations were able to undergo epidermal differentiation as measured by markers specific for spinous (K1, K10, involucrin) and granular layers (loricrin, filaggrin) (Figure 3H). Surprisingly, although relatively rare, some cells were even positive for AE13, specific for hair keratins. This ability was retained even by ninth passage cultures (shown).

Basal and Suprabasal Bulge-Derived Keratinocytes Possess Characteristics of Multipotent Stem Cells: Clonal Analyses and Engraftments

We next addressed whether the known ability of bulge cells to give rise to both epidermis and hair follicles is due to multipotency or to the existence of different unipotent bulge SC residents. Wild-type (WT) newborn mouse keratinocytes can generate epidermis, hair, and sebaceous glands if first combined with newborn dermal fibroblasts and then grafted to the back of a nude mouse at a site where the skin has been surgically removed (Lichti et al., 1993, Weinberg et al., 1993). Nude mice lack hairs because they are deficient for a matrix transcription factor required for hair differentiation (Nehls et al., 1994; Segre et al., 1995). The degree of SC self-renewal in vitro enabled us to generate sufficient numbers of K14-GFP-actin-positive $\alpha6^{low}CD34^{high}$ or $\alpha6^{high}CD34^{high}$ keratinocytes derived from single isolated bulge cells to permit such in vivo engraftment studies. Consequently, we took progeny derived from single GFP+ holoclones, combined them with newborn WT dermal cells, and then grafted the mixture onto the backs of nude mice.

As previously reported, grafts of dermal fibroblasts alone were able to produce a dermis that could support the inward migration of the nude mouse's keratinocytes, which then stratified and terminally differentiated (Figure 4A, left; Lichti et al., 1993; Weinberg et al., 1993). Some variability in surface contour was observed (e.g., Figure 4A', left), as would be expected from dermal scarring; however, the regenerated skin displayed a nude phenotype and lacked a fur coat (Figures 4A and 4A', left frames). By contrast, grafts containing GFP+ descendents from single $\alpha6^{low}CD34^{high}$ or $\alpha6^{high}CD34^{high}$ bulge cells exhibited tufts of hairs as well as epidermis (Figures 4A and 4A', middle and right frames). Fluorescence imaging revealed GFP+, which extended to but not beyond the boundaries of the graft (Figure 4B).

Immunofluorescence microscopy of skin sections revealed a marked contribution of GFP+ bulge descendants within each skin epithelial lineage (Figures 4C–4E). The brightest GFP fluorescence was seen in the epidermis, ORS, and sebaceous glands where the K14 promoter is most active. Longer exposure revealed GFP fluorescence in the transiently amplifying progenitor cells of the IRS (AE15+) and hair shaft, both readily discernable within grafts. Remarkably, grafts examined after the completion of their first hair cycle even displayed CD34+, K14-GFP+ cells at the follicle base (Figures 4F and 4G). Within longer-term grafts, evidence of at least one additional round of hair cycling was apparent.

No obvious abnormalities were detected in the morphology of the GFP+ epidermis, sebaceous glands, and hair follicles. GFP fluorescence was not detected in skin derived from nude or WT mice, nor was it detected in nonepithelial cell compartments, e.g., blood vessels or dermis, in which the K14 promoter was not active.

Both Basal and Suprabasal Bulge Cells Express Certain Molecular Signatures of Stemness

Recently, two groups reported partially overlapping ($\sim$30%) sets of $\sim$150 genes whose expression is preferentially upregulated in telogen phase bulge keratinocytes relative to keratinocytes residing outside the bulge (Tumbar et al., 2004; Morris et al., 2004). To identify which genes are upregulated in bulge SCs irrespective of their attachment to basal lamina and regardless of activation state, we isolated mRNAs from FACS-purified bulge populations during resting (7 weeks) and growing (4 weeks) phases of the first postnatal hair cycle and performed microarray analyses. mRNAs were scored as upregulated if their levels were greater than two times relative to the All GFP fraction of keratinocytes. RT-PCR on these and independent samples of fractionated mRNAs validated the quality of our databases (Figure 6 and data not shown).

(C) FACS analysis of BrdU LRCs (R1) demonstrating that LRCs obtained from in vivo BrdU pulse-chase analyses also exist as $\alpha6^{low}CD34^{high}$ and $\alpha6^{high}CD34^{high}$ subpopulations.

(D) Analysis of surface levels of $\alpha6$ and CD34 in K14-GFP-actin fractions from mice whose follicles were in telogen/early anagen, day 20; full anagen, day 28; or telogen, 7 weeks.

(E) FACS analysis of K14-GFP-actin expression in All GFP, $\alpha6^{low}CD34^{high}$, and $\alpha6^{high}CD34^{high}$ subpopulations.

(F) Expression of $\alpha6$, $\beta1$, K14-GFP-actin, and CD34 within All GFP, $\alpha6^{low}CD34^{high}$, and $\alpha6^{high}CD34^{high}$ subpopulations as determined by FACS analysis. Graph represents the geometrical mean channel fluorescence of the populations analyzed. Unsorted and FACS-sorted cells isolated on the basis of relative K14-GFP-actin, $\alpha6$ integrin, and CD34 surface levels were also subjected to cytospin and immunofluorescence. Note: $\alpha6^{low}CD34^{high}$ and $\alpha6^{high}CD34^{high}$ are positive for basal markers K5 and K15 but negative for differentiation markers K1, K6, and AE15.
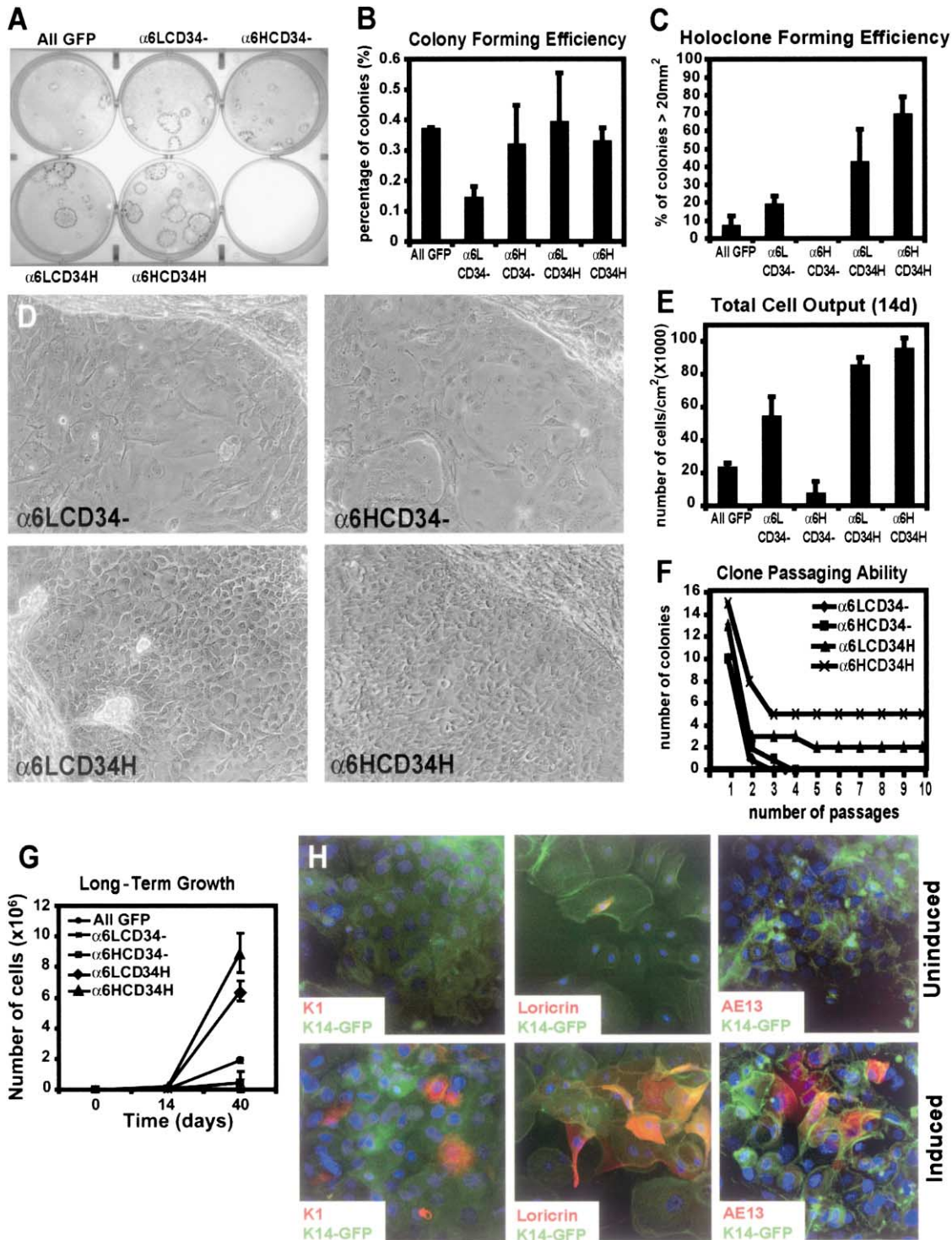
Figure 3. Basal and Suprabasal Bulge Cells Display Self-Renewal and Other Stem Cell Characteristics when Removed from their Niche and Placed in Culture

FACS-sorted keratinocytes from 28-day-old K14-GFP-actin mice were cultured 2 weeks in vitro and either fixed and stained with Rhodamine B for visual inspection (A), or trypsinized and counted for colony- and holoclone-forming efficiency analyses (B and C), or passaged for long-term survival and growth analyses (F and G). Passaged cells derived from individual bulge holoclones were also examined under normal (uninduced) or differentiation-stimulatory (induced) culture conditions. Shown in (H) are ninth passage GFP-actin-expressing cultures (green) after processing for immunofluorescence microscopy with antibodies (Texas red secondary antibodies) against epidermal (K1, loricrin) and hair-specific (AE13) differentiation markers. For all experiments, cultures were prepared in triplicate and experiments conducted greater than or equal to three times. Note: large colonies in primary CD34$^-$ cultures (derived from single cells outside the bulge) typically had differentiated morphologies and did not yield holoclones upon passage. In contrast, large colonies in primary CD34$^+$ cultures (derived from single cells within the bulge) displayed holoclone morphology and generated additional holoclones upon passage.
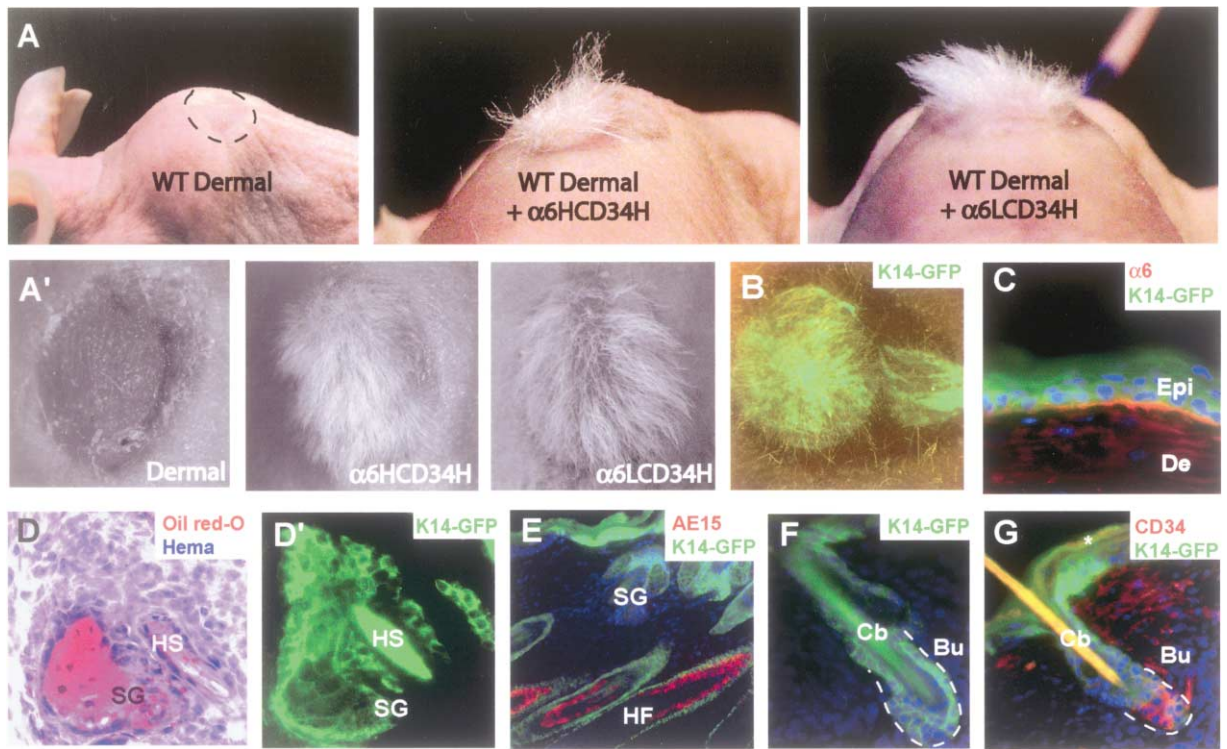
Figure 4. Clonal Analyses of Cells Derived from Single Bulge Cells: Self-Renewal and Multipotency In Vivo

WT (non-GFP) fibroblasts ± cloned, GFP-actin-expressing keratinocytes derived from single bulge cells were subjected to full thickness replacement grafting onto back skins of nude mice. After 3 weeks, grafts were photographed in regular (A, A′) or GFP fluorescence-sensitive lighting (B) and then processed either for fluorescence microscopy to examine contributions to skin SC lineages (C–G) or hematoxylin and oil-red-O staining to demonstrate end-stage sebaceous gland secretions (D). For microscopy, epifluorescent GFP was used in conjunction with antibodies against α6 integrin (C), the IRS follicle marker AE15 (E), or the bulge SC marker CD34 (G). Notes: (1) the K14 promoter used to drive GFP-actin is active in the bulge, and GFP-actin had a half-life sufficient to detect epifluorescence in all progeny of the bulge. Variability in GFP-actin levels arises from promoter downregulation in lineages of hair and IRS but is readily detected in their matrix progenitor cells. (2) GFP-actin keratinocyte-formed follicles not only possessed a CD34$^+$ niche but also underwent hair cycling (see, e.g., anagen in [E] and telogen in [F] and [G]), indicating self-renewal as well as multipotency in vivo.

Consistent with the bulge location of our α6^{high}CD34^{high} and α6^{low}CD34^{high} populations, the list of mRNAs upregulated in either of these compartments encompassed 80%–90% of mRNAs found to be upregulated in at least one of the previously published bulge databases (Tumbar et al., 2004; Morris et al., 2004). This said, a significant number of mRNAs were differentially expressed in the two populations, suggesting that the location of cells within the bulge markedly influenced the program of gene expression (Tables 1 and 2). Additionally, other mRNAs were upregulated in either telogen or anagen but not both. When pared to consider mRNAs upregulated in both telogen and anagen phases and in both basal and suprabasal compartments, a short list of key genes defining bulge cell characteristics emerges. We surmise that this list of only 56 upregulated mRNAs may constitute a molecular signature of bulge cells within their niche (Figure 5, top). Because these genes were upregulated in all bulge SC comparisons made to date, the SC niche environment appeared to be more critical to their expression than to attachment to basal lamina or hair cycle stage.

Table 1. Differences in Expression for Cell Division-Related Genes for Basal and Suprabasal Bulge SCs versus Total Epidermis

	α6^{high}CD34^{high} versus All GFP (Anagen/Telogen)	α6^{low}CD34^{high} versus All GFP (Anagen/Telogen)
Genes upregulated	Cdkn1b (P27) (2×/nf), Igfbp3 (3×/nf), Igfbp5 (14×/6×), Igfbp6 (5×/6×), Igfbp7 (6×/4×)	Cdkn1b (P27) (2×/nf), Cdkn2b (P15) (3×/5×)
Genes downregulated	cyclin A2 (4×/4×), cyclin B1 (10×/8×), cyclin B2 (9×/5×), cyclin D1 (2×/nf), cyclin D2 (3×/4×), Cdc2a (4×/8×), Cdc25c (4×/nf), Cdc6 (3×/2×), Cdc7 (4×/3×), Cdca1 (4×/3×), Chek1 (4×/5×), Cdkn1a (9×/3×), Cdkn2b (P15) (2×/nf), Wee1 (3×/4×), Pcna (2×/2×), Mki67 (10×/10×)	cyclin A2 (9×/5×), cyclin B1 (30×/14×), cyclin B2 (19×/4×), cyclin D1 (nf/7×), cyclin D2 (12×/18×), Cdc2a (27×/13×), Cdc25c (11×/nf), Cdc6 (4×/6×), Cdc7 (6×/4×), Cdca1 (13×/11×), Chek1 (7×/7×), Chek2 (4×/3×), Cdkn1a (3×/nf), Wee1 (3×/5×), Pcna (2×/2×), Mki67 (200×/26×)

Abbreviation: the times-fold changes are indicated in parentheses for anagen and telogen (anagen/telogen).
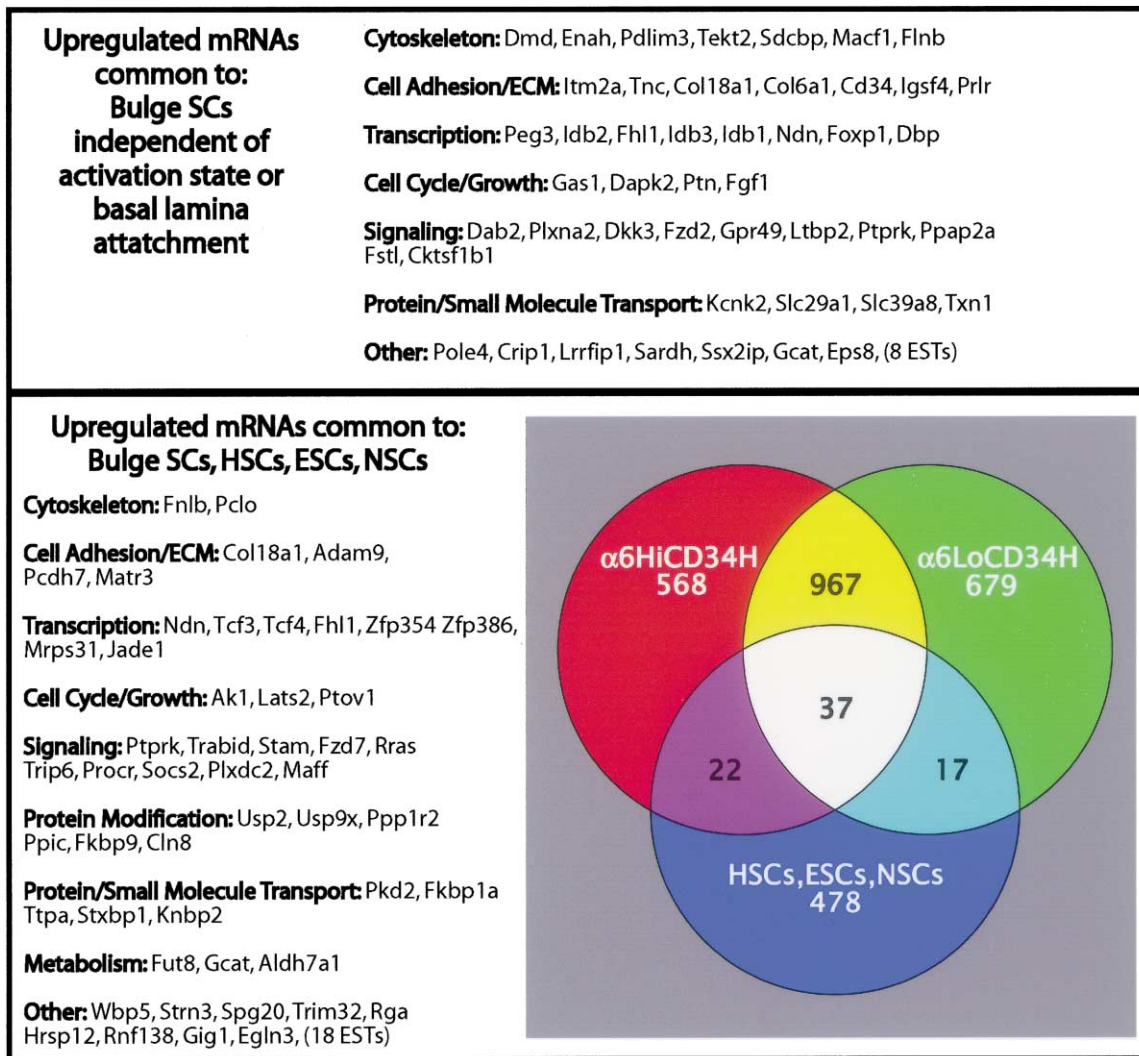
Upregulated mRNAs common to: Bulge SCs independent of activation state or basal lamina attachment	**Cytoskeleton:** Dmd, Enah, Pdlim3, Tekt2, Sdcbp, Macf1, Flnb
	Cell Adhesion/ECM: Itm2a, Tnc, Col18a1, Col6a1, Cd34, Igsf4, Prlr
	Transcription: Peg3, Idb2, Fhl1, Idb3, Idb1, Ndn, Foxp1, Dbp
	Cell Cycle/Growth: Gas1, Dapk2, Ptn, Fgf1
	Signaling: Dab2, Plxna2, Dkk3, Fzd2, Gpr49, Ltbp2, Ptprk, Ppap2a Fstl, Cktsf1b1
	Protein/Small Molecule Transport: Kcnk2, Slc29a1, Slc39a8, Txn1
	Other: Pole4, Crip1, Lrrfip1, Sardh, Ssx2ip, Gcat, Eps8, (8 ESTs)

**Upregulated mRNAs common to:
Bulge SCs, HSCs, ESCs, NSCs**

Cytoskeleton: Fnlb, Pclo

Cell Adhesion/ECM: Col18a1, Adam9, Pcdh7, Matr3

Transcription: Ndn, Tcf3, Tcf4, Fhl1, Zfp354 Zfp386, Mrps31, Jade1

Cell Cycle/Growth: Ak1, Lats2, Ptov1

Signaling: Ptprk, Trabid, Stam, Fzd7, Rras Trip6, Procr, Socs2, Plxdc2, Maff

Protein Modification: Usp2, Usp9x, Ppp1r2 Ppic, Fkbp9, Cln8

Protein/Small Molecule Transport: Pkd2, Fkbp1a Ttpa, Stxbp1, Knbp2

Metabolism: Fut8, Gcat, Aldh7a1

Other: Wbp5, Strn3, Spg20, Trim32, Rga Hrsp12, Rnf138, Gig1, Egln3, (18 ESTs)

Figure 5. A Stemness List for Bulge Cells and Comparisons with Other Stem Cell Types

Our duplicate microarrays from four bulge ($\alpha6^{high}$CD34^{high} and $\alpha6^{low}$CD34^{high}, telogen and anagen phase) and two All GFP-actin keratinocyte arrays were compared, and ~200 of 22,000 probe sets scored as upregulated by greater than or equal to two times in eight of eight bulge datasets. Fifty-six of these (shown) were also upregulated in previously published array datasets (Tumbar et al., 2004; Morris et al., 2004) (top). Many of the others were below the sensitivity limits of prior arrays. Our eight bulge cell datasets were also compared with other published SC databases (either Ivanova et al. [2002] or Ramalho-Santos et al. [2002]) for the overlap between hematopoietic stem cells (HSCs), embryonic stem cells (ESCs), and neural stem cells (NSCs) (bottom). The Venn diagram demonstrates the degree of overlap between basal and suprabasal bulge SCs and other SC databases. Note that ~14% of previously identified stemness genes overlapped with our bulge datasets.

By employing an approximately two times larger oligonucleotide array than previous bulge analyses, we could identify which upregulated bulge mRNAs are also preferentially upregulated in hematopoietic stem cells (HSCs), embryonic stem cells (ESCs), and neuronal stem cells (NSCs) (Ivanova et al., 2002; Ramalho-Santos et al., 2002). It is noteworthy that ~14% of mRNAs upregulated in HSCs, ESCs, and NSCs were also upregulated in either basal or suprabasal bulge SCs (Figure 5, bottom).

These comparisons further delineate a short list of stemness genes that now encompasses SCs isolated from a wide array of tissues. Several genes remaining on this short list continue to stand out as possible candidates to play a role in self-renewal and differentiation, including those involved in Wnt signaling (e.g., Tcfs and Fzd7), adhesion (e.g., Cadherin7, Collagen18a1, and

Adam9), and transcriptional regulation (e.g., Tcfs, Necdin, and four and a half LIM domain). In contrast, other mRNAs, including the one encoding the ABCG2 transporter protein that excludes Hoechst dye 33342 in HSCs and some other SCs (Zhou et al., 2001), did not appear to be enriched in $\alpha6^{high}$CD34^{high} bulge SCs and were actually downregulated in the $\alpha6^{low}$CD34^{high} SCs. This was consistent with our observation that CD34$^+$ bulge SCs were not enriched by Hoechst dye exclusion and in this regard differed from HSCs (data not shown; see also Triel et al. [2004]).

Relation between the Quiescence of Bulge Cells and the Stem Cell Niche

Whether in anagen or telogen, both bulge cell populations exhibited reduced mRNA levels for markers of pro-
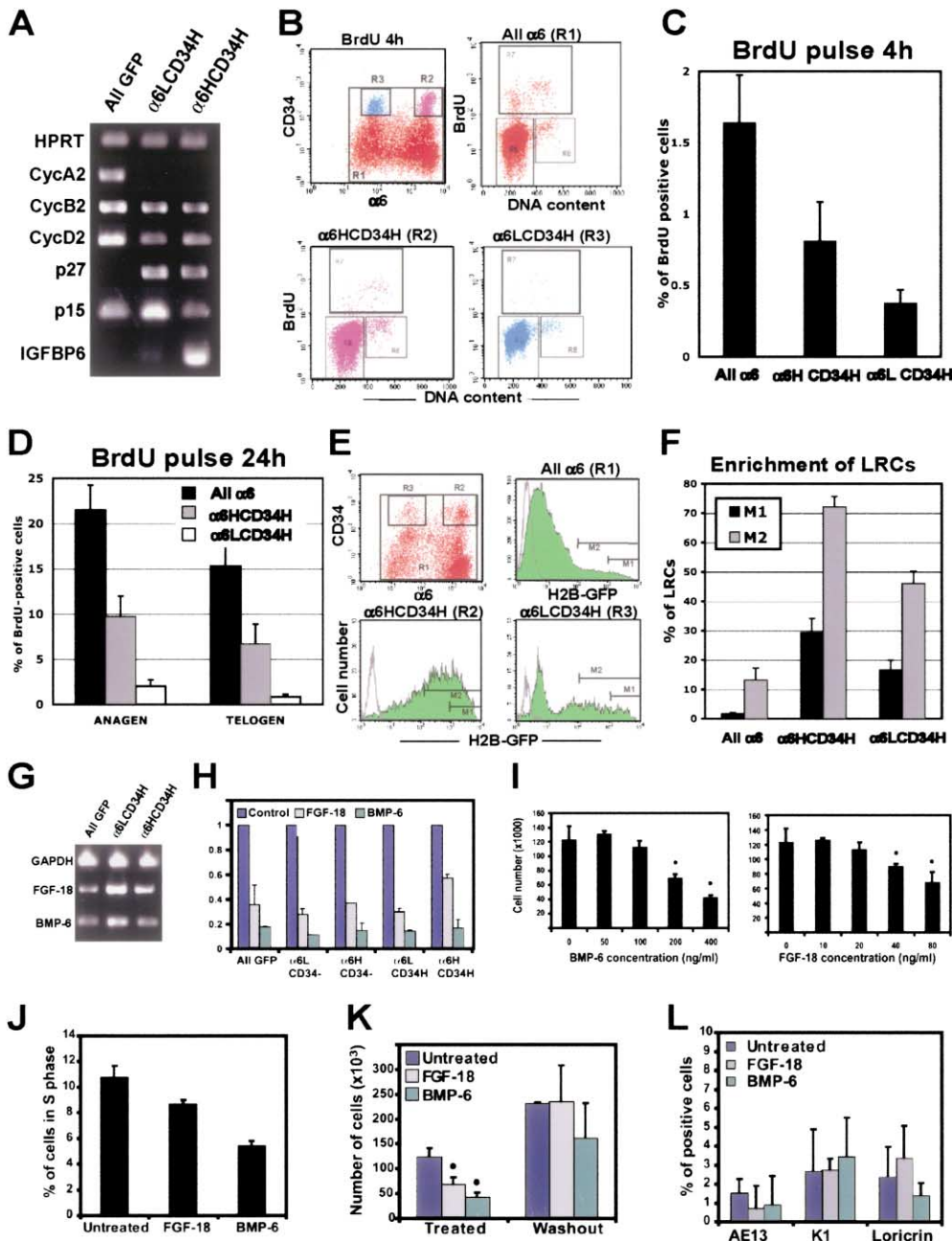
Figure 6. The Cycling Properties of Bulge Cells and their Relation to the Stem Cell Niche

(A) Semiquantitative RT-PCR of representative cell cycle genes found to be differentially expressed in keratinocytes within versus outside the bulge. Note downregulation of cyclins and upregulation of cell cycle inhibitory genes.

(B and C) K14-GFP-actin mice were injected with BrdU for 4 hr, and keratinocytes were analyzed by FACS for α6 and CD34 and for BrdU incorporation (S phase) and DNA content (Go/G1 versus G2/M). Shown are FACS profiles and gates and quantification of data (R2, α6^{high}CD34^{high}; R3, α6^{low}CD34^{high}; R1, All α6).

(D) Experiments were repeated as in (B) and (C), except BrdU labeling was for 24 hr and conducted at either 4 weeks (anagen) or 7 weeks (telogen). Note that mitoses within the bulge were more frequent for cells attached to the basal lamina.

(E and F) Enrichment of H2B-GFP LRCs in CD34$^+$ bulge subpopulations. Postnatal day 28 TRE-H2B-GFP/K5-tet^{off} mice were fed doxycycline for 4 weeks (chased). Their keratinocytes were gated and analyzed as above, but, in addition, cells were scored for retention of histone-GFP fluorescence (M1 and M2 represent two different levels of label retention).

(G) Semiquantitative RT-PCR of genes encoding BMP-6 and FGF-18, two of only three growth factors/ligands preferentially upregulated in the slowest cycling bulge compartment (α6^{low}CD34^{high}, see above).

(H) Effects of 80 ng/ml FGF-18 and 400 ng/ml BMP-6 on proliferation of colonies formed from FACS-sorted, K14-GFP-actin keratinocyte populations. After 14 days, cells from triplicate experiments were counted and the data plotted as treated cells relative to untreated control cells from each population (individually normalized to 1).

(I) Dose response of FGF-18 and BMP-6 on keratinocyte growth.

(J) FACS analyses of cell cycle profiles from keratinocytes treated 10 days after plating for 24 hr either with FGF-18 or BMP-6.

(K) Reversibility of growth-inhibitory effects of FGF-18 and BMP-6. Cells were treated as in (H), but, this time, cells were washed three times with PBS and cultured an additional 2 days in the absence of the growth inhibitory factors. Triplicate plates of cells were counted before and after the washout.

(L) Effects of FGF-18 and BMP-6 on terminal differentiation. After treating cells as in (H), immunofluorescence microscopy was conducted with antibodies against K1, AE13, and involucrin.

Table 2. Difference in Expression of Adhesion, Extracellular Matrix, Cytoskeletal, and Growth-Related Genes Upregulated in the Bulge between Basal and Suprabasal SCs

	Fold Change between α6^{high}CD34^{high} and α6^{low} CD34^{high} (Anagen/Telogen)	Fold Change between α6^{low}CD34^{high} and α6^{high}CD34^{high} (Anagen/Telogen)
Adhesion- and membrane-related proteins	Necl1 (16×/17×), Sema3e (16×/3×), Trpv4 (14×/11×), Bgn (13×/nf), Glrb (9×/5×), Calcrl (9×/15×), Itm2a (7×/6×), Cspg (5×/3×), Alcam (4×/5×), Itm2c (3×/3×)	Aqp5 (35×/26×), Pvrl4 (16×/13×), Pmp22 (8×/8×), Ramp1 (4×/16×), Nope (3×/2×), Sema4g (2×/3×)
Growth-related proteins	Ctgf (26×/16×), Ltbp1 (18×/15×), Igfbp5 (14×/4×), Igfbp7 (7×/6×), Sparc (12×/13×), Unc3 (10×/2×), Cxcl14 (4×/2×), Gdf10 (3×/2×), Kitl (2×/3×), Fgfr1 (3×/3×), Tnfrsf1 1b (5×/3×), Itb6 (5×/3×)	Bmp6 (4×/12×), Sectm1 (3×/5×), FGF-18 (7×/12×), Cdkn2b (8×/8×)
Extracellular matrix	Col4a1 (10×/6×), Col4a2 (10×/6×), Col7a1 (7×/5×), Col18a1 (2×/nf), Vit (14×/8×), Npnt (5×/7×), Fbln2 (3×/3×), Mmp2 (9×/5×)	Col3a1 (41×/65×), Fbn2 (13×/5×), Fn1 (6×/4×)
Cytoskeleton	Myoc (8×/6×)	Dcamkl1 (43×/21×), Sncg (6×/4×), Pak3 (5×/3×), Kif5c (5×/6×), Gphn (3×/3×)

Abbreviation: the times-fold changes are indicated in parentheses for anagen and telogen (anagen/telogen).

liferation, such as Ki67 and PCNA, and cell cycle progression, such as cyclins (D2, A2, B1, and B2) (Table 1; Figure 6A). Conversely, p27 (cdkn1b), an inhibitor of cyclin E-Cdk2, was upregulated in the bulge relative to the rest of epidermis, as were several members of the IGFBP family (e.g., Igfbp3, 5, 6, and 7), which bind and sequester insulin growth factor, a potent stimulant of epidermal proliferation (Vasioukhin et al., 2001; Bennett et al., 2003). Thus, the slow-cycling nature of bulge cells appears at least in part to be governed by transcriptional changes, a mechanism not typically implicated in cell cycle control.

To address whether the proliferative status of bulge cells depends upon basal lamina attachment as it does for basal epidermal cells, we first employed BrdU labeling to examine the relative number of S phase cells in the two compartments of anagen phase, 4-week-old back skin follicle bulges. FACS analyses revealed fewer BrdU-labeled cells in each of the two bulge populations than in their epidermal counterparts (Figures 6B and 6C). However, noticeably fewer suprabasal bulge cells were labeled than basal bulge cells. This difference was also seen with longer BrdU pulses and with telogen phase as well as anagen phase follicles (Figures 6C and 6D). From these data, we conclude that bulge cells can proliferate during the hair cycle but do so to a lesser extent than other proliferative cells in the epidermis and its appendages. As in the epidermis, basal lamina attachment appeared to influence proliferative status within the bulge.

To assess the history of cell divisions, we used TRE-H2BGFP/K5Tet^{off} transgenic mice to determine how the two bulge populations dilute histone-GFP protein when expression is shut off for 4 weeks at the start of the first postnatal hair cycle. As expected, both populations were enriched for LRCs when compared to their epidermal counterparts (Figures 6E and 6F). However, suprabasal bulge cells displayed less fluorescence than basal bulge cells. Together, these data suggested that suprabasal cells may undergo more divisions than their basal counterparts, and yet, once they enter their suprabasal location, they cycle less frequently. This finding

underscores the quiescent state of the niche and is consistent with the notion that suprabasal bulge cells may be derived from their basal counterparts.

A search for possible factors that might contribute to the growth inhibitory state of bulge cells uncovered FGF-18 and BMP-6 as two of only three mRNAs encoding ligands that were substantially upregulated in suprabasal bulge cells (Table 2 and Figure 6G). FGF-18 transcript levels were also higher overall within the bulge than outside this niche. Since both bulge populations expressed mRNAs encoding their corresponding membrane receptors, we examined how primary bulge keratinocyte colonies respond to these factors.

Both FGF-18 and BMP-6 inhibited growth of all keratinocytes tested, irrespective of location within skin epithelium (Figure 6H). The inhibitory effects occurred in a dose-dependent fashion (Figure 6I), and cell cycle profiles showed an S phase reduction in the treated cultures (Figure 6J). Despite signs of reduced proliferation, the effects were largely reversible (Figure 6K). Moreover, treatment with these factors did not appear to appreciably induce terminal differentiation relative to control cultures, as judged by colony morphology and biochemical markers (Figure 6L). When taken together with the previously noted upregulation of TGFβ pathway members in the bulge (Tumbar et al., 2004; Morris et al., 2004), these data provide new insights into mechanisms by which the specialized, reversible growth inhibitory environment of the bulge may be generated.

Discussion

Self-Renewal and Multipotency of Skin Stem Cells
Recent studies provided compelling evidence that SCs reside within the bulge and that bulge cell descendants contribute to hair follicles and sebaceous glands in normal homeostasis and to epidermis after injury (Taylor et al., 2000; Oshima et al., 2001; Tumbar et al., 2004; Morris et al., 2004). However, the defining features of SCs, namely self-renewal and multipotency, necessitated clonal analysis, previously precluded because of difficulties faced in culturing adult murine keratinocytes.

By refining conditions to permit generation of holoclones from individual bulge cells, we learned that, with additional passages, holoclones give rise to increasing numbers of holoclones, thereby demonstrating that self-renewal of these cells can take place in vitro. Moreover, when grafted in vivo, holoclone descendants derived from a single bulge cell gave rise not only to epidermis but also to multiple hair follicles and sebaceous glands. The ability to generate follicles persisted even after multiple passages of bulge cell descendants in serum-rich medium favoring a wound, i.e., epidermal-promoting state. These new data now document that keratinocytes derived from individual bulge cells possess the classical defining features of bona fide SCs.

A Role for Bulge SCs in Organizing and Maintaining their Niche

The molecular mechanisms underlying the formation of stem cell niches are largely unknown (Spradling et al., 2001; Lin, 2002; Fuchs et al., 2004). Thus, we were intrigued to detect GFP$^+$, CD34$^+$ cells at the base of the telogen phase follicles that developed from engraftments of GFP$^+$, bulge SC-derived holoclone cells. Moreover, since new hairs were seen in the grafts following the first postgraft hair cycle, some of the graft-generated follicles appeared to possess functional SCs. These new results suggest that, when grafted, multipotent bulge SCs may be able to participate in reassembling a niche, even when they are temporarily removed and expanded in culture. The data are provocative in context of the bulge-preferred expression of mRNAs encoding factors stimulatory to the dermal sheath and sensory neurons that surround the niche (Tumbar et al., 2004; Morris et al., 2004; this study). Together, they may be indicative of an impact of SCs not only on assembling but also on maintaining their bulge niche microenvironment and architecture. The extent to which this fascinating phenomenon may extend to other SCs remains to be determined.

Asymmetry and Differential Gene Expression within the SC Niche

A bulge in the ORS endows the follicle SC niche with its name. This structure appears at the start of the first postnatal hair cycle, when the newly forming hair germ grows downward to one side of the symmetrical cup of CD34$^+$, label-retaining cells that encase the remnant club hair. Although SCs must be present at earlier times in order to initiate the hair cycle and presumably to participate in wound repair, the formation of the physical structure of the follicle SC niche is a postnatal event.

Our studies revealed that the formation of the bulge is accompanied by internal movements and a revamping of SC niche architecture. This results in the development of suprabasal cells, creating an asymmetry within the niche. The existence of a suprabasal bulge layer is intriguing in that it provides a potential mechanism for setting up the unique and defining architecture of the hair follicle. Precisely how bulge SCs are able to execute the distinct programs of terminal differentiation within the hair follicle continues to be a mystery. However, like the basal layer of the bulge, the ORS cells maintain their attachment to an underlying basal lamina.

By contrast, the cells of the concentric cylinders that constitute the companion layer, the IRS, and the hair shaft are not associated with a basement membrane. Although the relation between basal and suprabasal compartments remains to be established, it is possible that, through their generation, some of the spatial features necessary for commitment to these lineages may already be met within the SC niche. The differences in gene expression between basal and suprabasal bulge cells is consistent with this concept. As additional microarray analyses are conducted on keratinocyte populations purified from different stages of hair lineage determination, it should become clearer as to whether suprabasal bulge cells could represent quiescent early progeny of basal bulge stem cells.

In addition to these tantalizing parallels, the defining features of bulge SCs also included a surprising number of genes encoding cell adhesion and cytoskeletal components, as well as extracellular matrix components. These attributes suggest an architecture uniquely suited to the dual ability of SCs to adhere to their residence and yet be mobilized to exit the niche during wound repair or upon activation of the hair cycle. That some of these genes were selectively upregulated in anagen versus telogen lends further support to this notion. Thus, although some features of the differential expression program within the bulge were suggestive of an early commitment stage, others appeared more reflective of an asymmetry designed for responses of bulge SCs to various external cues.

The Impact of the Niche on SC Behavior

The similarities of the two bulge compartments were as revealing as their differences. In addition to their label-retaining properties, upregulated mRNAs common to the two populations suggested an ability of the niche to influence gene expression, irrespective of whether the SCs were attached to or detached from basement membrane and irrespective of whether the hair follicle was in a growing or resting stage. The most conspicuous molecular signatures of the bulge transcriptional profile were mRNAs encoding proteins that are inhibitory for growth and/or terminal differentiation. The downregulation of mRNAs encoded by cell cycle-regulated genes suggested a hitherto unexplored regulatory mechanism underlying the quiescent state of SCs. The expression of factors such as FGF-18 and BMP-6 in the bulge and their ability to slow keratinocyte growth in vitro without inducing expression of terminal differentiation provides a mechanism for placing bulge SCs in a holding pattern, able to maintain a quiescent state and yet still primed to respond to growth and/or differentiation cues imposed by changes in the microenvironment.

Despite the impact of the niche, both populations behaved analogously when removed from this location and placed in culture medium. Although some of these similarities may be attributable to their placement in a common new environment, other behavioral responses seemed intrinsic. An example was the generation of relatively undifferentiated holoclones, more prevalent within cultures derived from bulge SCs than in adult murine keratinocytes cultured from regions outside the bulge. It was also notable that cultured cells derived

from single bulge SCs from either compartment were able to produce epidermis, hair follicles, and sebaceous glands in engraftments. Thus, despite the substantial differences in gene expression underlying these two populations in vivo, the cells nevertheless retained their potential to become bona fide stem cells after passaging in vitro and grafting in vivo.

We cannot rule out the possibility that culture conditions can elicit reprogramming of otherwise committed cells, as recently suggested by Li et al. (2004). If such changes occur in vitro, they could mask a lineage commitment step that might occur within the bulge SC niche. An unequivocal resolution to this issue will depend upon direct grafting of single bulge cells, which is currently beyond the scope of present technologies. However, our studies imply that, if reprogramming is required to maintain and/or regain multipotency of either population of bulge SCs, the critical commitment gene(s) should be responsive to and reversed by extrinsic cues, in this case imposed by culturing the cells.

Conclusions

By improving methods to isolate and culture murine bulge keratinocytes in vitro, we were able to demonstrate self-renewal of bulge cells in vitro and their multipotency in vivo. This provided definitive evidence for bulge cells as bona fide SCs. In addition, the procedure for isolating bulge cells on the basis of cell surface markers opens the door for analyses of bulge SCs from mutant mouse models. This method may also be useful for isolating human skin SCs, which are known to possess elevated $\alpha 6$ and CD34 levels (Tani et al., 2000; Poblet and Jimenez, 2003).

Our approaches have also allowed us to isolate bulge cells both from growing and resting phases of the hair cycle. By determining the specific genes whose expression is altered in both basal and suprabasal bulge layers and in anagen and telogen, we made inroads into refining the list of skin epithelial stemness genes and strengthened parallels to SCs found in other cell types. The data also yielded a new appreciation for the relation between SCs and their niche. Finally, in probing the heterogeneity within the follicle SC niche, we uncovered possible insights into the earliest stages, still reversible, at which bulge cells might first begin their journey toward hair follicle differentiation and/or orchestrate the formation of the concentric rings of distinct differentiation lineages within this structure.

Experimental Procedures

Mice and Labeling Experiments

TRE-H2B-GFP/K5Tet^{off} and K14 GFP-actin mice were generated previously (Vaezi et al., 2002; Tumbar et al., 2004). For H2B-GFP pulse-chase experiments, 4-week (pulse period) TRE-H2B-GFP/K5Tet^{off} mice were fed with doxycycline for 4–5 weeks (chase period). 5-Bromo-2′-deoxyuridine (BrdU) (Sigma-Aldrich) pulse-chase experiments were performed as described (Braun et al., 2003). Postnatal day 10 CD-1 mice were injected intraperitoneally with 50 μg/g BrdU two times per day for 2 days and analyzed 28 days later (chase period) for label retention. For cell cycle analysis, day 28 mice were injected once with 50 μg/g BrdU and analyzed 4 hr later for BrdU incorporation. Continuous BrdU administration was performed by adding BrdU to drinking water at a concentration of 0.8 mg/ml.

Histology and Immunofluorescence

Tissues were embedded in OCT, frozen, and sectioned. Paraformaldehyde-fixed sections were then subjected to immunofluorescence microscopy or hematoxylin staining essentially as described (Vaezi et al., 2002). When applicable, the MOM Basic Kit (Vector Laboratories) was used to prevent nonspecific binding of mouse monoclonal antibodies. The following antibodies and dilutions were used: $\alpha 6$-integrin (rat, 1:100, Pharmingen, BD Biosciences), CD34 (rat, 1:100, Pharmingen), K5 (rabbit, 1:5000, Fuchs Lab), K15 (rabbit, 1:1000, Fuchs Lab), K6 (rabbit, 1:1000, Fuchs Lab), BrdU (rat, 1:50, Abcam), S100a4 (rabbit, 1:300, Kizania Kenji; Basic Research Laboratories, Kanebo Ltd.), Dcamkl1 (rabbit, 1:300, Christopher Walsh, Beth Israel Deaconess Medical Center), and FITC or Texas red-conjugated anti-donkey or anti-goat antibodies (1:300, Molecular Probes). Nuclei were stained using 4′6′-diamidino-2-phenylindole (DAPI) for immunofluorescence and TOPRO-3 (Molecular Probes) for confocal microscopy. The three-dimensional reconstructions of confocal analysis were performed using LSM510 Confocal Analyzer (Zeiss) or Imaris softwares (Bitplane AG).

FACS Analysis

For each experiment, a scalpel was used to remove fat and underlying subcutis from the back skins of five adult K14-GFP-actin mice, and following trypsinization, neutralized cell suspensions were strained (70 μM, then 40 μM pores; BD Biosciences). Single cell suspensions in 2% FCS in PBS were then exposed for 30 min on ice to primary antibodies directly coupled with a fluorochrome or with Avidin. After washing two times with PBS, cells were incubated with Streptavidin coupled to specific fluochromes (1:200, Pharmingen) for 30 min and then washed and resuspended in PBS supplemented with 2% FCS and 300 ng/ml propium Iodide (Sigma-Aldrich).

Primary antibodies used for FACS analysis were anti-$\alpha 6$ integrin (CD49f) directly coupled to FITC, PE, or Cychrome (Pharmingen) and anti-CD34 coupled to biotin, FITC, or PE (Pharmingen), anti-$\beta 1$ integrin biotinylated (Pharmingen). BrdU detection was performed using BD Pharmingen BrdU Flow Kit (Pharmingen). Cell isolations were performed on a FACSVantage SE system equipped with FACS DiVa software (BD Biosciences). Epidermal cells were gated for single events and viability, then sorted according their expression of K14-actin GFP, $\alpha 6$-integrin, and CD34. Purity of sorted cells was determined by postsort FACS analysis and typically exceeded 95%. FACS analyses were performed either on FACSort or BD LSR (BD Biosciences). Cytospin analysis was done with a Cytospin4 unit (Thermo/Shandon) and stained as described earlier.

Cell Culture

Viability of FACS-isolated adult keratinocytes was assessed by trypan blue (Sigma) staining, and cell numbers were determined by hemocytometer. Equal numbers of live cells were plated onto mitomycin-treated 3T3 fibroblasts in E-media (Rheinwald and Green, 1977) supplemented with 15% serum and 0.3 mM calcium. After 14 days in vitro, cells were trypsinized and counted (Coulter counter; Beckman). To visualize colony number and morphology, cells were stained with 1% Rhodamine B (Sigma). For immunofluorescence, FACS-isolated cells were plated onto chamber slides. For expansion of particular colonies, individual holoclones were trypsinized in cloning cylinders and passaged onto a fresh feeder layer. To induce terminal differentiation, serum was reduced to 5%, and calcium was raised to 1.5 mM.

Engraftment Experiments

Engraftments were performed as described (Weinberg et al., 1993). Equal numbers of newborn dermal fibroblasts $\pm$ K14-GFP-actin epithelial cells ($\alpha 6^{low}$CD34^{high} or $\alpha 6^{high}$CD34^{high}) were combined at 10^4 cells/μl, and 500 μl was injected into a silicon chamber implanted onto the back of an anesthetized nude mouse (Jackson Laboratories). After 1 week, wounds had healed, and chambers were removed. Hair typically appeared 1–2 weeks thereafter.

RNA Isolation and Microarray Analysis

Cells were collected from FACS into lysis buffer, and total RNAs were purified using the Absolutely RNA Kit (Stratagene). mRNAs

were assessed by RNA 6000 Pico Assay (Agilent) and quantified spectrophotometrically. Primer olig0-dT-T7 (Genset) was used to reverse transcribe (SuperScript cDNA Synthesis Kit, Invitrogen) and then amplify (MessageAmp aRNA Kit, Ambion) 200 ng of RNA. Random priming and biotinylated nucleotides were used to obtain cRNA for microarray. After quality control (Agilent), 10 μg labeled cRNA was hybridized for 16 hr at 45°C to mouse genome array MOE430a (Affymetrix). Processed chips were then read by an argon-ion laser confocal scanner (Genomics Core Facility, MSKCC). The entire procedure was repeated in duplicate for each sample to produce two independent datasets per mRNA sample.

Microarray Data Analysis
Raw microarray images were quantified using Gene Chip Operating Software (GCOS, Affymetrix). The default analysis parameters and a target value intensity of 500 were employed. Results were then filtered to eliminate any change calls below two times (p > 0.01). Gene changes scored as increasing but called absent in the numerator, and any changes scored as decreased and called absent in the denominator were eliminated. Gene changes were confirmed by analyses of duplicate arrays. For comparative purposes, we converted MOE430a probe sets to equivalent probe sets on MGu74V2 Affymetrix arrays (MGu74V2A, B, C, 36,000 probe sets), employing GeneSpring (Silicon Genetics). Since only 22,000 probe sets could be directly compared, the common upregulated probe sets may underrepresent the actual overlap for databases acquired with larger probe sets.

Semiquantitative RT-PCR and Confirmation of Microarray Data
Total RNAs were purified from FACS-sorted cells as above, and, after quantification by Ribogreen labeling (Molecular Probes), normalized RNA quantities were reverse transcribed (Invitrogen). cDNAs were normalized by PCR amplification with primers to two housekeeping genes, HPRT and GAPDH. PCR amplification of sample targets was completed using primers designed to produce a product spanning exon/intron boundaries. Control amplifications with RNAs minus reverse transcriptase yielded no products for any of the primer pairs tested.

References

Barrandon, Y., and Green, H. (1987). Three clonal types of keratinocyte with different capacities for multiplication. Proc. Natl. Acad. Sci. USA *84*, 2302–2306.

Bennett, W.R., Crew, T.E., Slack, J.M., and Ward, A. (2003). Struc-tural-proliferative units and organ growth: effects of insulin-like growth factor 2 on the growth of colon and skin. Development *130*, 1079–1088.

Braun, K.M., Niemann, C., Jensen, U.B., Sundberg, J.P., Silva-Vargas, V., and Watt, F.M. (2003). Manipulation of stem cell proliferation and lineage commitment: visualisation of label-retaining cells in wholemounts of mouse epidermis. Development *130*, 5241–5255.

Cotsarelis, G., Sun, T.T., and Lavker, R.M. (1990). Label-retaining cells reside in the bulge area of pilosebaceous unit: implications for follicular stem cells, hair cycle, and skin carcinogenesis. Cell *61*, 1329–1337.

Fuchs, E., and Raghavan, S. (2002). Getting under the skin of epidermal morphogenesis. Nat. Rev. Genet. *3*, 199–209.

Fuchs, E., Tumbar, T., and Guasch, G. (2004). Socializing with the neighbors: stem cells and their niche. Cell *116*, 769–778.

Ivanova, N.B., Dimos, J.T., Schaniel, C., Hackney, J.A., Moore, K.A., and Lemischka, I.R. (2002). A stem cell molecular signature. Science *298*, 601–604.

Jahoda, C.A., Horne, K.A., and Oliver, R.F. (1984). Induction of hair growth by implantation of cultured dermal papilla cells. Nature *311*, 560–562.

Li, A., Pouliot, N., Redvers, R., and Kaur, P. (2004). Extensive tissue-regenerative capacity of neonatal human keratinocyte stem cells and their progeny. J. Clin. Invest. *113*, 390–400.

Lichti, U., Weinberg, W.C., Goodman, L., Ledbetter, S., Dooley, T., Morgan, D., and Yuspa, S.H. (1993). In vivo regulation of murine hair growth: insights from grafting defined cell populations onto nude mice. J. Invest. Dermatol. *101*, 124S–129S.

Lin, H. (2002). The stem-cell niche theory: lessons from flies. Nat. Rev. Genet. *3*, 931–940.

Martin, K.H., Slack, J.K., Boerner, S.A., Martin, C.C., and Parsons, J.T. (2002). Integrin connections map: to infinity and beyond. Science *296*, 1652–1653.

Morris, R.J., and Potten, C.S. (1999). Highly persistent label-retaining cells in the hair follicles of mice and their fate following induction of anagen. J. Invest. Dermatol. *112*, 470–475.

Morris, R.J., Liu, Y., Marles, L., Yang, Z., Trempus, C., Li, S., Lin, J.S., Sawicki, J.A., and Cotsarelis, G. (2004). Capturing and profiling adult hair follicle stem cells. Nat. Biotechnol. *22*, 411–417.

Nehls, M., Pfeifer, D., Schorpp, M., Hedrich, H., and Boehm, T. (1994). New member of the winged-helix protein family disrupted in mouse and rat nude mutations. Nature *372*, 103–107.

Oshima, H., Rochat, A., Kedzia, C., Kobayashi, K., and Barrandon, Y. (2001). Morphogenesis and renewal of hair follicles from adult multipotent stem cells. Cell *104*, 233–245.

Panteleyev, A.A., Jahoda, C.A., and Christiano, A.M. (2001). Hair follicle predetermination. J. Cell Sci. *114*, 3419–3431.

Poblet, E., and Jimenez, F. (2003). CD34 in human hair follicle. J. Invest. Dermatol. *121*, 1220.

Potten, C.S. (1974). The epidermal proliferative unit: the possible role of the central basal cell. Cell Tissue Kinet. *7*, 77–88.

Potten, C.S., and Morris, R.J. (1988). Epithelial stem cells in vivo. J. Cell Sci. Supp. *10*, 45–62.

Ramalho-Santos, M., Yoon, S., Matsuzaki, Y., Mulligan, R.C., and Melton, D.A. (2002). "Stemness": transcriptional profiling of embryonic and adult stem cells. Science *298*, 597–600.

Rheinwald, J.G., and Green, H. (1977). Epidermal growth factor and the multiplication of cultured human epidermal keratinocytes. Nature *265*, 421–424.

Rochat, A., Kobayashi, K., and Barrandon, Y. (1994). Location of stem cells of human hair follicles by clonal analysis. Cell *76*, 1063–1073.

Segre, J.A., Nemhauser, J.L., Taylor, B.A., Nadeau, J.H., and Lander, E.S. (1995). Positional cloning of the nude locus: genetic, physical, and transcription maps of the region and mutations in the mouse and rat. Genomics *28*, 549–559.

Spradling, A., Drummond-Barbosa, D., and Kai, T. (2001). Stem cells find their niche. Nature *414*, 98–104.

Tani, H., Morris, R.J., and Kaur, P. (2000). Enrichment for murine keratinocyte stem cells based on cell surface phenotype. Proc. Natl. Acad. Sci. USA *97*, 10960–10965.

Taylor, G., Lehrer, M.S., Jensen, P.J., Sun, T.T., and Lavker, R.M. (2000). Involvement of follicular stem cells in forming not only the follicle but also the epidermis. Cell *102*, 451–461.

Triel, C., Vestergaard, M.E., Bolund, L., Jensen, T.G., and Jensen, U.B. (2004). Side population cells in human and mouse epidermis lack stem cell characteristics. Exp. Cell Res. *295*, 79–90.

Tumbar, T., Guasch, G., Greco, V., Blanpain, C., Lowry, W.E., Rendl, M., and Fuchs, E. (2004). Defining the epithelial stem cell niche in skin. Science *303*, 359–363.

Vaezi, A., Bauer, C., Vasioukhin, V., and Fuchs, E. (2002). Actin cable dynamics and Rho/Rock orchestrate a polarized cytoskeletal architecture in the early steps of assembling a stratified epithelium. Dev. Cell *3*, 367–381.

Vasioukhin, V., Bauer, C., Degenstein, L., Wise, B., and Fuchs, E. (2001). Hyperproliferation and defects in epithelial polarity upon conditional ablation of α-catenin in skin. Cell *104*, 605–617.

Wagers, A.J., and Weissman, I.L. (2004). Plasticity of adult stem cells. Cell *116*, 639–648.

Watt, F.M. (2002). Role of integrins in regulating epidermal adhesion, growth and differentiation. EMBO J. *21*, 3919–3926.

Weinberg, W.C., Goodman, L.V., George, C., Morgan, D.L., Ledbetter, S., Yuspa, S.H., and Lichti, U. (1993). Reconstitution of hair follicle development in vivo: determination of follicle formation, hair growth, and hair quality by dermal cells. J. Invest. Dermatol. *100*, 229–236.

Weissman, I.L., Anderson, D.J., and Gage, F. (2001). Stem and progenitor cells: origins, phenol-types, lineage commitments, and transdifferentiations. Annu. Rev. Cell Dev. Biol. *17*, 387–403.

Werb, Z. (1997). ECM and cell surface proteolysis: regulating cellular ecology. Cell *91*, 439–442.

Zhou, S., Schuetz, J.D., Bunting, K.D., Colapietro, A.M., Sampath, J., Morris, J.J., Lagutina, I., Grosveld, G.C., Osawa, M., Nakauchi, H., and Sorrentino, B.P. (2001). The ABC transporter Bcrp1/ABCG2 is expressed in a wide variety of stem cells and is a molecular determinant of the side-population phenotype. Nat. Med. *7*, 1028–1034.